5-31-2018

Kelvin-Mach Wake in a Two-Dimensional Fermi Sea

Eugene B. Kolomeisky
University of Virginia

Joseph P. Straley
University of Kentucky, jstraley@uky.edu

Kelvin-Mach Wake in a Two-Dimensional Fermi Sea

Digital Object Identifier (DOI)
https://doi.org/10.1103/PhysRevLett.120.226801

Notes/Citation Information
Published in *Physical Review Letters*, v. 120, issue 22, 226801, p. 1-5.

Kelvin-Mach Wake in a Two-Dimensional Fermi Sea

Eugene B. Kolomeisky[1] and Joseph P. Straley[2]
[1]Department of Physics, University of Virginia, P. O. Box 400714, Charlottesville, Virginia 22904-4714, USA
[2]Department of Physics and Astronomy, University of Kentucky, Lexington, Kentucky 40506-0055, USA

(Received 22 December 2017; published 31 May 2018)

The dispersion law for plasma oscillations in a two-dimensional electron gas in the hydrodynamic approximation interpolates between $\Omega \propto \sqrt{q}$ and $\Omega \propto q$ dependences as the wave vector q increases. As a result, downstream of a charged impurity in the presence of a uniform supersonic electric current flow, a wake pattern of induced charge density and potential is formed whose geometry is controlled by the Mach number M. For $1 < M \leq \sqrt{2}$, the wake consists of transverse wave fronts confined within a sector, whose angle is given by the classic Mach condition. An additional wake of a larger angle resembling the Kelvin ship wake, and consisting of both transverse and diverging wave fronts, is found outside the Mach sector for $M > \sqrt{2}$. These wakes also trail an external charge, traveling supersonically, a fixed distance away from the electron gas.

DOI: 10.1103/PhysRevLett.120.226801

An object uniformly moving, relative to a medium, gives rise to a series of effects ranging from the formation of a Mach shock wave cone behind a supersonic projectile [1] and Cherenkov radiation emitted by a rapidly moving charge [2], to the creation of wakes on a water surface by ships [3]. One feature that these effects have in common is that the interaction between the object and the medium triggers the coherent emission of collective excitations of the medium, which combine constructively to form the wake [4]. Here, we describe the coherence effect wherein plasma waves, emitted by a two-dimensional (2D) electron gas, form a wake pattern resembling both Mach and ship wakes [3]. Hereafter, we speak of the electron gas; the theory for the gas of holes is the same.

The starting point of our analysis is an expression for the dynamical dielectric function of the 2D electron gas in the hydrodynamic approximation, which, neglecting the effects of dissipation and retardation, is given by [5,6]:

$$\epsilon(\omega, \mathbf{q}) = \frac{\omega^2 - \Omega^2(\mathbf{q})}{\omega^2 - s^2 q^2}, \tag{1}$$

where ω is the frequency, $\Omega(\mathbf{q})$ is the frequency of plasma oscillations as a function of the wave vector $\mathbf{q}$,

$$\Omega^2(\mathbf{q}) = gq + s^2 q^2, \tag{2}$$

and $q = |\mathbf{q}|$. This description encompasses systems ranging from those whose electrons obey parabolic [5,6] to linear (graphene) dispersion laws [7]. The material parameters, $g = 2\pi n e^2 v_F^2/\kappa\zeta(n)$ (a characteristic acceleration) and $s = v_F(\partial p/\partial\varepsilon)^{1/2}$ (the speed of sound), are determined by the equilibrium electron number density n, the equation of state in the neutral limit [entering via the density dependence of the chemical potential $\zeta(n)$ and the energy density dependence of the pressure $p(\varepsilon)$], the background dielectric constant κ, and the limiting (Fermi) velocity v_F [8].

In the long-wavelength limit $\mathbf{q} \to 0$, the spectrum (2) is formally the same as that of gravity waves on deep water, $\Omega^2(\mathbf{q}) = gq$ [3] (where, in this context, g is the free-fall acceleration), an observation due to Dyakonov and Shur [9]. Since plasma oscillations are classical in nature [8], a series of effects analogous to classical waves on water are then expected in electron layers.

One of the most familiar manifestations of the $\Omega(\mathbf{q}\to 0) \propto \sqrt{q}$ dispersion law in fluid mechanics is the Kelvin wake that trails a traveling pressure source: the 39° angle of the wake is independent of the source velocity and has a characteristic "feathered" pattern [3]. One then might infer that an external charge traveling nonrelativistically, a fixed distance away from the plane of the electron system, disturbs the latter in the form of an "electron" Kelvin wake. Such a conclusion was recently made in the literature in the context of doped graphene [10]; it is misleading because it overlooks a crucial deviation from the strict $\sqrt{q}$ dispersion law. The same criticism applies to a conjecture that a stationary Kelvin wake should be formed downstream from a defect in the 2D electron gas in the presence of a current [11]. A wake is formed behind a moving source whenever there is a mode whose phase velocity matches the speed of the source [the precise statement is given by Eq. (9) below]. For a strictly $\sqrt{q}$ dispersion law, such a mode can always be found no matter what the speed of the source. However, the spectrum of plasma oscillations (2) deviates from the $\sqrt{q}$ law, and the phase velocity Ω/q is always above the speed of the sound s, which is thus the critical velocity for wake formation in 2D electron systems. If the acceleration g in Eq. (2) were zero, the wake pattern would resemble that formed behind a

supersonic projectile, with a wake angle determined by the Mach number $M = v/s$ [1], where v is the speed of the source. For a finite Mach number, one would then expect a pattern sharing features of both the Kelvin and Mach wakes, hereafter called the Kelvin-Mach wake.

In an earlier study, Fetter [6] has analyzed various aspects of the electromagnetic response of an electron layer to a moving charge. However, the problem was solved in the Fourier representation, and the real space pattern of the induced charge and potential were not addressed.

Our goal is to solve for the geometry of the wake induced by the moving charge. This is done by focusing on the case when the external charge is in the plane of the electron system. Since only the relative motion of the charge and the medium matters, in practice, this situation can be realized by subjecting an electron layer with an embedded Coulomb impurity to a supersonic current flow.

Supersonic flows are experimentally accessible, as we will now show.

The speed of sound s is less than the Fermi velocity v_F, but it typically has the same order of magnitude.

For a parabolic dispersion law, it can be estimated as $s \simeq v_F \simeq c(m_0/137m)a_B\sqrt{n}$, where m_0 is the electron mass in a vacuum and a_B is the Bohr radius. For $m_0/m = 10$ and $n = 10^{12}\,\mathrm{cm}^{-2}$, the speed of sound can be estimated as $s \simeq 10^6\,\mathrm{cm/s}$. This large value can be attained at a low temperature, where the mobility can be as large as $10^4\ \mathrm{cm}^2/(\mathrm{V\,s})$ [5]. The required electric field would be $10^2\ \mathrm{V/cm}$, which is five orders of magnitude smaller than the dielectric breakdown field of the SiO_2 insulating layer, common to various practical realizations of electron layer systems [5].

Similarly, in graphene (a linear dispersion material), the Fermi velocity is two orders of magnitude smaller than the speed of light, but the electron mobility is of the order $10^5\ \mathrm{cm}^2/(\mathrm{V\,s})$ [12], which translates into a $10^3\ \mathrm{V/cm}$ electric field needed to propel graphene's electrons past the speed of sound. There exists direct experimental evidence [13] that the saturation velocity in graphene on SiO_2 above room temperature exceeds $3 \times 10^7\ \mathrm{cm/s}$ at a low carrier density, while the intrinsic graphene saturation velocity could be more than twice the quoted value.

The ratio $d = s^2/g$ (the Debye screening length of the electron gas [5]) sets the length scale of the effects to be discussed. It is of the order 10^{-6} cm (and weakly doping dependent) in materials with a parabolic dispersion law [5] and of the order $\kappa/\sqrt{n}$ in graphene [12].

There is a further advantage of studying graphene rather than the electron layers of the past [5]. Charged impurities can be embedded into graphene in a controlled manner [14], and high-resolution, noninvasive imaging of charge currents in graphene structures [15] can be employed to directly observe the electron Kelvin-Mach wake; in other systems, the formation of the wake can only be inferred indirectly from the onset of nonzero wave resistance.

We will be studying the electromagnetic response of an electron layer to an external potential $\varphi_{\mathrm{ext}}(\mathbf{r}, t)$, where $\mathbf{r}$ is the position within the layer and t is the time; the dependence on these quantities is in response to an external charge (number) density $n_{\mathrm{ext}}(\mathbf{r}, t)$. Their Fourier transformations are related by the Coulomb law $\varphi_{\mathrm{ext}}(\omega, \mathbf{q}) = 2\pi e n_{\mathrm{ext}}(\omega, \mathbf{q})/\kappa q$ [5,6]. According to the linear response theory, the Fourier components of the induced density $n_{\mathrm{in}}(\omega, \mathbf{q})$ and induced potential $\varphi_{\mathrm{in}}(\omega, \mathbf{q})$ are given by

$$n_{\mathrm{in}}(\omega, \mathbf{q}) = \left(\frac{1}{\epsilon(\omega, \mathbf{q})} - 1\right) n_{\mathrm{ext}}(\omega, \mathbf{q}) = \frac{g q n_{\mathrm{ext}}(\omega, \mathbf{q})}{\omega^2 - \Omega^2(\mathbf{q})}, \tag{3}$$

$$\varphi_{\mathrm{in}}(\omega, \mathbf{q}) = \left(\frac{1}{\epsilon(\omega, \mathbf{q})} - 1\right) \varphi_{\mathrm{ext}}(\omega, \mathbf{q}) = \frac{2\pi e g}{\kappa} \frac{n_{\mathrm{ext}}(\omega, \mathbf{q})}{\omega^2 - \Omega^2(\mathbf{q})}. \tag{4}$$

Inverting the Fourier transformations, we find the electromagnetic response in the direct space and time representation

$$n_{\mathrm{in}}(\mathbf{r}, t) = g \int \frac{d^2 q d\omega}{(2\pi)^3} \frac{q n_{\mathrm{ext}}(\omega, \mathbf{q}) e^{i(\mathbf{q}\cdot\mathbf{r} - \omega t)}}{(\omega + i0)^2 - \Omega^2(\mathbf{q})}, \tag{5}$$

$$\varphi_{\mathrm{in}}(\mathbf{r}, t) = \frac{2\pi e g}{\kappa} \int \frac{d^2 q d\omega}{(2\pi)^3} \frac{n_{\mathrm{ext}}(\omega, \mathbf{q}) e^{i(\mathbf{q}\cdot\mathbf{r} - \omega t)}}{(\omega + i0)^2 - \Omega^2(\mathbf{q})}, \tag{6}$$

where ω in the denominators of the integrands is endowed with an infinitesimally small, positive imaginary part ($\omega \to \omega + i0$) to guarantee the analyticity of the integrands in the upper half plane of complex ω [2]. A unit external charge, moving with a constant velocity $\mathbf{v}$ within the layer, is described by $n_{\mathrm{ext}}(\mathbf{r}, t) = \delta(\mathbf{r} - \mathbf{v}t)$, whose Fourier transformation is $n_{\mathrm{ext}}(\omega, \mathbf{q}) = 2\pi\delta(\omega - \mathbf{q}\cdot\mathbf{v})$. Substituting this into Eqs. (5) and (6), and changing the frame of reference to that of the charge, $\mathbf{r} - \mathbf{v}t \to \mathbf{r}$, we find

$$n_{\mathrm{in}}(\mathbf{r}) = g \int \frac{d^2 q}{(2\pi)^2} \frac{q e^{i\mathbf{q}\cdot\mathbf{r}}}{(\mathbf{q}\cdot\mathbf{v} + i0)^2 - \Omega^2(\mathbf{q})}, \tag{7}$$

$$\varphi_{\mathrm{in}}(\mathbf{r}) = \frac{2\pi e g}{\kappa} \int \frac{d^2 q}{(2\pi)^2} \frac{e^{i\mathbf{q}\cdot\mathbf{r}}}{(\mathbf{q}\cdot\mathbf{v} + i0)^2 - \Omega^2(\mathbf{q})}. \tag{8}$$

This is the electrodynamic response of the electron layer having an initially uniform flow velocity $-\mathbf{v}$ to a point Coulomb impurity of a unit charge fixed at the origin or, equivalently, to a traveling charge in the comoving reference frame.

For $\mathbf{v} = 0$, Eqs. (7) and (8) describe the static screening response of the electron layer to a point charge [5,6]. Slow motion ($v < s$) brings anisotropy to the response, but no other qualitative changes occur because the denominators of the integrands in Eqs. (7) and (8) cannot vanish for $\mathbf{q}$ real; the $+i0$ frequency shift in the integrands is unimportant. This

regime, where no plasma waves are emitted, will be discussed elsewhere. However, when v exceeds the speed of sound, the denominators of the integrands in Eqs. (7) and (8) can vanish; integrals (7) and (8) are dominated by the real wave vectors $\mathbf{q}$, given by the solutions to

$$\Omega(\mathbf{q}) = \pm \mathbf{q} \cdot \mathbf{v}. \tag{9}$$

The response pattern is now qualitatively different, and the presence of the $+i0$ shift is required to supply a rule for bypassing the poles of the integrands in Eqs. (7) and (8). This regime is our focus. For the special case of a charge moving through a medium, with a velocity exceeding the phase velocity of light, the condition (9) is encountered in the theory of the Cherenkov effect [2]. In its general form, Eq. (9) was given by Landau as a threshold for the emission of elementary excitations by a superfluid flowing along a capillary [16].

The theory is linear, the source has zero range, and the wake is stationary in the reference frame of the source. Then, dimensional analysis implies that the spatial scale of the pattern can only depend on the parameters of the spectrum g and s (2), and the velocity of the source v: (i) For $s = 0$ (the Kelvin wake), the only parameter having dimensions of length that can be formed out of g and v is the characteristic length scale of the wake, $\lambda = v^2/g$. Measuring the length in units of λ, density in units of $1/\lambda^2$, and potential in units of $e/\kappa\lambda$ eliminates all of the parameters from the problem. Thus, all Kelvin wakes are geometrically similar. While this argument does not supply the value of the wake angle, it does predict that it is independent of v and g. (ii) For $s \neq 0$ (the Kelvin-Mach wake), two independent length scales can be formed out of the parameters of the problem: $\lambda = v^2/g$ and $d = s^2/g$ (the Debye screening length). Their ratio, $\lambda/d = v^2/s^2 = M^2$, is the square of the Mach number; once this is fixed, either λ or d may be used to characterize the length scale of the wake. Measuring the length in units of d, the density in units of $1/d^2$, and the potential in units of $e/\kappa d$ eliminates all of the parameters from the problem, except for the Mach number. Thus, all the Kelvin-Mach wakes of the same Mach number $M = v/s$ are geometrically similar.

Even though the Fourier integrals (7) and (8) cannot be computed in a closed form, the geometry of the wake pattern can be inferred with the help of Kelvin's method of stationary phase [3]. The idea is that when the phase factor $f = \mathbf{q} \cdot \mathbf{r}$ in the integrands in (7) and (8) varies rapidly with q, the exponentials are highly oscillatory so that contributions from various elements d^2q cancel each other; this is the case of destructive interference with almost zero net result. This cancelation, however, will not occur for the wavelengths for which f is stationary with respect to $\mathbf{q}$ [which is additionally restricted by the Cherenkov-Landau condition (9)]; this is the case of constructive interference. Since the integrands of the induced charge (7) and potential (8) differ by a smooth factor of q, the two wake patterns have the same geometry.

Let us choose the positive x direction along the velocity vector $\mathbf{v}$ and measure length in units of the Debye screening length $d = s^2/g$. The trace of the external charge divides the plane into two regions related to one another by reflection; without the loss of generality, we can focus on the $y > 0$ half-space. Here, the wake is formed by a superposition of the waves, whose wave vectors have positive components, $q_{x,y} > 0$. Then the phase $f = \mathbf{q} \cdot \mathbf{r}$ is given by

$$f = \frac{\{2(M^2-1)q_y^2 + 1 + [1 + 4(M^2-1)M^2q_y^2]^{1/2}\}^{1/2}}{(M^2-1)\sqrt{2}}\, x + q_y y, \tag{10}$$

where instead of q_x, we substituted the positive solution of the Cherenkov-Landau equation (9) corresponding to the plasma spectrum (2). Direct inspection of Eq. (10) shows that the condition of stationary phase $df/dq_y = 0$ can only be satisfied for $x < 0$, which is where the wake is. In terms of a new variable $z = [1 + 4(M^2-1)M^2q_y^2]^{1/2} \geq 1$, the expression for the phase (10) can be transformed into

$$f = \frac{(z^2-1)^{1/2}}{2M(M^2-1)^{1/2}}\left[\frac{(z-1+2M^2)^{1/2}}{(M^2-1)^{1/2}(z-1)^{1/2}}x + y\right]. \tag{11}$$

The condition of the stationary phase $f'(z) = 0$ now becomes

$$-\frac{y}{x} = \frac{1}{(M^2-1)^{1/2}}\frac{(z-1)^{1/2}(z+M^2)}{z(z-1+2M^2)^{1/2}}. \tag{12}$$

Since the phase f is constant along the wave front, Eqs. (11) and (12) can be solved relative to x and y to give the equation for the wave front in a parametric form:

$$x(z) = \frac{2f(M^2-1)}{M}\frac{z(z-1+2M^2)^{1/2}}{(z+1)^{3/2}}, \tag{13}$$

$$y(z) = -\frac{2f(M^2-1)^{1/2}}{M}\frac{(z+M^2)(z-1)^{1/2}}{(z+1)^{3/2}}. \tag{14}$$

We now see that internal consistency of the argument requires the phase to be negative, $f < 0$.

As in Kelvin's case [3], the range of applicability of the method of stationary phase limits our analysis to large distances r from the source, which in the original units of length means $r \gg d = s^2/g$.

To put the consequences of Eqs. (12)–(14) into perspective, we begin with the Kelvin case $s = 0$, which corresponds to $M = \infty$. In this limit, Eq. (12) simplifies to

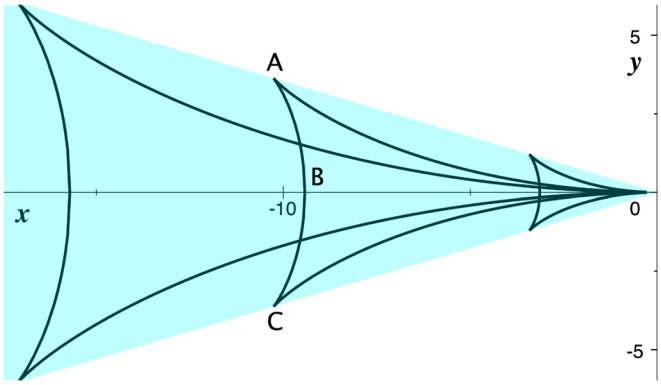

FIG. 1. Wave fronts of the Kelvin wake, Eq. (16), with the source at the origin traveling to the right. The wake is confined within the shaded light blue 39° wedge; the unit of length is $\lambda = v^2/g$.

$$-\frac{y}{x} = \frac{(z-1)^{1/2}}{\sqrt{2}z}, \tag{15}$$

whose right-hand side vanishes at $z = 1$, $z \to \infty$, and reaches a maximum value of $1/2\sqrt{2}$ in between. Therefore, the equation of the stationary phase (15) has one solution for $-y/x = 0$, two solutions for $0 < -y/x < 1/2\sqrt{2}$ coalescing at $-y/x = 1/2\sqrt{2}$, and none for $-y/x > 1/2\sqrt{2}$. The angle between the wake edges is $2\arctan(1/2\sqrt{2}) \approx 39°$, which is Kelvin's classic result [3].

In order to take the Kelvin $s = 0$ limit in Eqs. (13) and (14), we temporarily restore the original units of length, $(x, y) \to (x, y)/d = (g/s^2)(x, y)$, followed by selecting $\lambda = v^2/g$ as a new unit of length with the result

$$x(z) = \frac{2\sqrt{2}fz}{(z+1)^{3/2}}, \qquad y(z) = -\frac{2f(z-1)^{1/2}}{(z+1)^{3/2}}. \tag{16}$$

A series of these wave fronts is shown in Fig. 1, where, for the purpose of illustration, we chose $f = -2\pi(l + 1/2)$, $l = 0, 1, 2$; the $y < 0$ part of the wake is obtained by reflection. The wake consists of the so-called transverse wave fronts ABC, connecting the edges of the pattern across the central line $y = 0$, and the diverging wave fronts AO and CO, connecting the source at the origin to the edges of the pattern [3]. The two wave fronts meet at A and C at the edges of the pattern.

For a finite M, the right-hand side of Eq. (12) vanishes at $z = 1$ and approaches $(M^2 - 1)^{-1/2}$ as $z \to \infty$; the intermediate behavior depends on the Mach number: (i) When $1 < M \leq \sqrt{2}$, the right-hand side of Eq. (12) is a monotonically increasing function of z. Thus, the equation of stationary phase (12) has one (transverse) solution for $0 \leq -y/x < (M^2 - 1)^{-1/2}$ and none for $-y/x \geq (M^2 - 1)^{-1/2}$. Therefore, the angle of the wake is $2\arctan(M^2 - 1)^{-1/2}$, which is Mach's classic result [1]. A series of wave fronts,

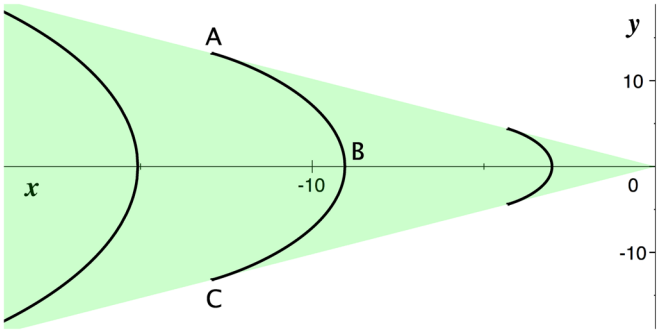

FIG. 2. Wave fronts of the Kelvin-Mach wake for $1 < M \leq \sqrt{2}$, Eqs. (13) and (14), with an external charge at the origin traveling to the right. The wake consists of transverse wave fronts confined within shaded light green Mach sector of angle $2\arctan(M^2 - 1)^{-1/2}$, the unit of length is the Debye screening length $d = s^2/g$, and $M = 1.4$ was employed to produce the drawing.

(13) and (14), employing the same choice for the phase f as in Fig. 1, is shown in Fig. 2. The wake consists of transverse wave fronts ABC connecting the edges of the pattern. We stress that in view of the dispersion relation (2), the wake is *not* the classic Mach wake; the wave fronts of the latter, $y/x = \pm(M^2 - 1)^{-1/2}$, coincide with its geometrical boundary [1]. (ii) When $M > \sqrt{2}$, the right-hand side of Eq. (12) has a maximum $(M^2+1)^{3/2}/(2M^2-1)^{3/2}$ at $z=(2M^2-1)/(M^2-2)$. Now the equation of stationary phase (12) has one (transverse) solution for $0 \leq -y/x < (M^2 - 1)^{-1/2}$, two (transverse and diverging) solutions for $(M^2 - 1)^{-1/2} \leq -y/x < (M^2 + 1)^{3/2}/(2M^2 - 1)^{3/2}$ coalescing at $-y/x = (M^2 + 1)^{3/2}/(2M^2 - 1)^{3/2}$, and none for $-y/x > (M^2 + 1)^{3/2}/(2M^2 - 1)^{3/2}$. The wake pattern shown in Fig. 3 is confined within a sector of angle

$$\phi(M) = 2\arctan\frac{(M^2+1)^{3/2}}{(2M^2-1)^{3/2}} \tag{17}$$

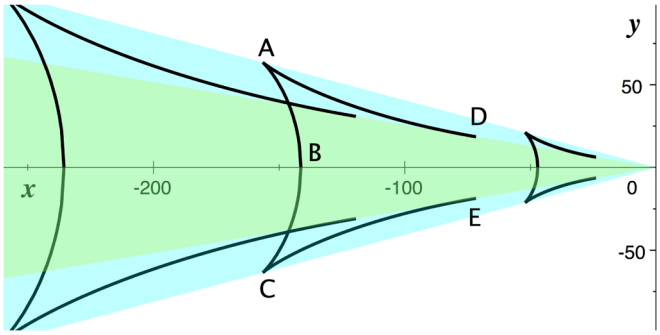

FIG. 3. Same as in Fig. 2 for $M > \sqrt{2}$. Additionally, both transverse and diverging wave fronts are present in the region shaded light blue outside the Mach sector. The angle of the wake is given by Eq. (17), and $M = 4$ was employed to produce the drawing.

that is wider than Mach's. In addition to the transverse wave fronts ABC connecting the edges of the pattern, the diverging wave fronts, AD and CE, are also found outside the Mach (light green) sector; the region with two types of wave fronts present is shaded light blue. In contrast to the Kelvin wake (Fig. 1), divergent wave fronts connect the edges of the Kelvin-Mach wake to the boundaries of the Mach sector, a consequence of the $z \to \infty$ limit of Eqs. (12)–(14). As M increases, the Mach sector becomes narrow, closing as $M \to \infty$, while the wake angle (17) decreases, approaching Kelvin's limit of $\phi(\infty) = 2\arctan(1/2\sqrt{2})$. It is expected that the appearance of the diverging wave fronts for $M > \sqrt{2}$ will be accompanied by a noticeable increase of the wave resistance.

To summarize, our analysis has uncovered intricate wake patterns that can be produced in 2D electron systems that we hope will be observed in future experiments.

We thank G. Rousseaux and M. I. Dyakonov for informing us of Refs. [4,11], and M. I. Dyakonov and E. Y. Andrei for valuable comments.

[1] L. D. Landau and E. M. Lifshitz, *Fluid Mechanics* (Pergamon, Oxford, 1987), Sec. 82.
[2] L. D. Landau and E. M. Lifshitz, *Electrodynamics of Continuous Media* (Pergamon, Oxford, 1984), Secs. 82 and 115.
[3] H. Lamb, *Hydrodynamics* 6th ed. (Cambridge University Press, Cambridge, 1975), Chap. IX.
[4] For a review of different types of wakes see I. Carusotto and G. Rousseaux, in *Analogue Gravity Phenomenology*, edited by D. Faccio *et al.*, Lecture Notes in Physics (Springer, Cham, 2013), p. 109, DOI: 10.1007/978-3-319-00266-8_6.
[5] T. Ando, A. B. Fowler, and F. Stern, Rev. Mod. Phys. **54**, 437 (1982), and references therein.
[6] A. L. Fetter, Ann. Phys. (N.Y.) **81**, 367 (1973).
[7] E. H. Hwang and S. Das Sarma, Phys. Rev. B **75**, 205418 (2007); S. Das Sarma and E. H. Hwang, Phys. Rev. Lett. **102**, 206412 (2009).
[8] E. B. Kolomeisky and J. P. Straley, Phys. Rev. B **96**, 165116 (2017).
[9] M. Dyakonov and M. Shur, Phys. Rev. Lett. **71**, 2465 (1993).
[10] X. Shi, X. Lin, F. Gao, H. Xu, Z.Yang, and B. Zhang, Phys. Rev. B **92**, 081404(R) (2015); A. J. Chaves, N. M. R. Peres, G. Smirnov, and N. A. Mortensen, Phys. Rev. B **96**, 195438 (2017).
[11] M. I. Dyakonov, in *Future Trends in Microelectronics: Journey into the Unknown*, edited by S. Luryi, J. Xu, and A. Zaslavsky (John Wiley and Sons, New York, 2016), p. 113.
[12] A. H. C. Neto, F. Guinea, N. M. R. Peres, K. S. Novoselov, and A. K. Geim, Rev. Mod. Phys. **81**, 109 (2009).
[13] V. E. Dorgan, M.-H. Bae, and E. Pop, Appl. Phys. Lett. **97**, 082112 (2010).
[14] J. Mao, Y. Jiang, D. Moldovan, G. Li, K. Watanabe, T. Taniguchi, M. R. Masir, F. M. Peeters, and E. Y. Andrei, Nat. Phys. **12**, 545 (2016).
[15] J.-P. Tetienne, N. Dontschuk, D. A. Broadway, A. Stacey, D. A. Simpson, and L. C. L. Hollenberg, Sci. Adv. **3**, e1602429 (2017).
[16] L. Landau, J. Phys. **5**, 71 (1941); I. M. Khalatnikov, *An Introduction to the Superfluidity* (Perseus, Cambridge, MA, 2000), Chap. 1.